The EMBO Journal vol.15 no.10 pp.2547–2555, 1996

Multiple roles for divalent metal ions in DNA transposition: distinct stages of Tn*10* transposition have different Mg^{2+} requirements

Murray S.Junop and David B.Haniford[1]

Department of Biochemistry, University of Western Ontario, London, Ontario N6A 5B7, Canada

[1]Corresponding author

Tn*10* transposition takes place by a non-replicative mechanism in which the transposon is excised from donor DNA and integrated into a target site. Mg^{2+} is an essential cofactor in this reaction. We have examined the Mg^{2+} requirements at various steps in Tn*10* transposition. Results presented here demonstrate that Tn*10* excision can occur efficiently at a 16-fold lower Mg^{2+} concentration than strand transfer and that, at Mg^{2+} concentrations in the range of 60-fold below the wild-type optimum, double strand cleavage events at the two transposon ends are completely uncoupled. These experiments identify specific breakpoints in Tn*10* transposition which are sensitive to Mg^{2+} concentration. Whereas the uncoupling of double strand cleavage events at the two transposon ends most likely reflects the inability of two separate IS10 transposase monomers in the synaptic complex to bind Mg^{2+}, the uncoupling of transposon excision from strand transfer is expected to reflect either a conformational change in the active site or the existence of an Mg^{2+} binding site which functions specifically in target interactions. We also show that Mn^{2+} relaxes target specificity in Tn*10* transposition and suppresses a class of mutants which are blocked specifically for integration. These observations can be explained by a model in which sequence-specific target site binding is tightly coupled to a conformational change in the synaptic complex which is required for catalysis of strand transfer.

Keywords: divalent metal ions/DNA transposition/protein–DNA complex/relaxed specificity/transposase

Introduction

Transposons are mobile genetic elements. Their mobilization plays an important role in shaping the structures of the genomes in which they reside. Mechanistic details of transposition reactions have been best worked out for a number of different prokaryotic transposons. In these systems, transposition takes place through multi-step reaction pathways which are carried out by transposon-encoded transposase proteins and regulated to some degree by host proteins (reviewed in Haniford and Chaconas, 1992; Mizuuchi, 1992a). The basic steps mediated by bacterial transposase proteins are closely related to those mediated by the integrase proteins which direct retroviral/retrotransposon integration reactions (reviewed in Mizuuchi, 1992b; Craig, 1995; Polard and Chandler, 1995). Defining structure–function relationships for transposase and integrase proteins is a major focus of current studies and is expected to contribute significantly to our overall understanding of enzymatic mechanisms.

Tn*10* is a composite bacterial transposon (Figure 1) (reviewed in Kleckner, 1989). Transposition of this element occurs through a non-replicative mechanism in which the transposon is first excised from flanking donor DNA and then integrated into a new site (Bender and Kleckner, 1986; Haniford *et al.*, 1989; Benjamin and Kleckner, 1992). The site of integration is not random, as Tn*10* exhibits a strong preference for the sequence 5′GCTNAGC3′ (Halling and Kleckner, 1982). An early and necessary step in Tn*10* transposition involves the pairing of two transposon ends (Haniford *et al.*, 1991; Haniford and Kleckner, 1994; Sakai *et al.*, 1995). All of the chemical steps (excision and strand transfer) in Tn*10* transposition take place in the context of this 'paired end' or 'synaptic' complex (Sakai *et al.*, 1995). A similar requirement for end interactions has also been observed in bacteriophage Mu transposition (Craigie and Mizuuchi, 1987; Surette *et al.*, 1987; Mizuuchi *et al.*, 1992) and probably represents a general feature of transposition reactions. Excision of Tn*10* from the donor DNA involves an ordered set of strand cleavage events in which the transferred strands are first cut at both transposon ends producing a doubly nicked intermediate, followed by cleavage of the non-transferred strands (Bolland and Kleckner, 1995). Second strand cleavages at the two ends are not temporally coupled so that a single end break intermediate precedes the appearance of the excised transposon intermediate (Haniford and Kleckner, 1994; Sakai *et al.*, 1995). The 3′ OH ends of the excised transposon intermediate are then joined to 5′ PO_4 groups in the target DNA which are separated by nine residues and situated on opposite strands (Benjamin and Kleckner, 1992). Removal of the flanking donor DNA is required for successful target interactions (J.Sakai and N.Kleckner, personal communication).

Mg^{2+} is an essential cofactor in a large number of phosphoryl transfer reactions, including the chemical steps in Tn*10* transposition (Morisato and Kleckner, 1987). Structural studies on several protein–DNA complexes, including those formed by Klenow polymerase (Beese and Steitz, 1991), rat β polymerase (Pelletier *et al.*, 1994), *Eco*RI (Kim *et al.*, 1990) and *Eco*RV (Kostrewa and Winkler, 1995), have provided evidence that Mg^{2+} plays a direct role in the catalysis of the respective phosphoryl transfer reactions. In these as well as other proteins, including many transposases and integrases (Polard and Chandler, 1995), other restriction enzymes (Dorner and Schildkraut, 1994) and nucleases (Davies *et al.*, 1991), evidence has been provided indicating that acidic amino acids play a critical role in binding Mg^{2+} in the active

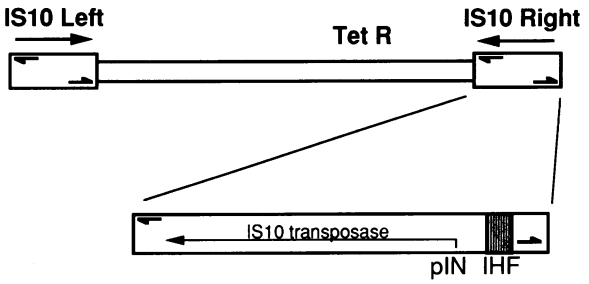

Fig. 1. Tn*10* is ~9.3 kb in length. It is made up of a tetracycline resistance determinant which is flanked by nearly identical copies of the insertion sequence IS10, which are present in inverted repeat orientation. IS10 Right encodes a 46 kDa transposase protein and is itself a fully functional transposition module. The DNA sites required for IS10 transposition are called outside and inside ends, as defined by their position relative to the tetracycline resistance determinant in Tn*10*. Outside and inside ends share a nearly perfect 23 bp terminal repeat sequence (small arrows) with which transposase makes its primary contacts (Kleckner *et al.*, 1995). In addition to this sequence, full outside end function requires IHF which binds to a site immediately adjacent to the 23 bp terminal repeat sequence (Huisman *et al.*, 1989). Transposition of a Tn*10* derivative containing two appropriately positioned inside ends can be carried out *in vitro* without a host factor, indicating that inside end function is host factor independent and that IS10 transposase protein possesses all of the biochemical activities necessary for a complete transposition reaction (Benjamin and Kleckner, 1992; Chalmers and Kleckner, 1994).

sites of these enzymes. Many transposase and retroviral integrase proteins contain a triad of acidic amino acids, known as the DDE motif, which is thought to participate in this function (Kulkosky *et al.*, 1992). In all of these systems, mutating these residues to amino acids without carboxylate side chains results in catalytically inactive proteins, as would be expected for residues which are important for catalysis (Kulkosky *et al.*, 1992; Van Gent *et al.*, 1992; Baker and Luo, 1994; Craig, 1995; Kim *et al.*, 1995; Polard and Chandler, 1995). In IS10 transposase, amino acids D97, D161 and E292 comprise the DDE motif. Mutations at these positions block the chemical steps in Tn*10* transposition without significantly affecting paired end complex formation (Bolland and Kleckner, 1996; Kennedy and Haniford, 1996). Mutations in acidic amino acids that are known to position Mg^{2+} ions for catalysis in the restriction endonuclease *Eco*RV, produce an analogous phenotype (Selent *et al.*, 1992). In addition, mutations in the MuA transposase DDE motif have essentially the same phenotype as the IS10 transposase DDE mutants (Baker and Luo, 1994; Kim *et al.*, 1995). More direct evidence for a role in Mg^{2+} binding for the MuA DDE residues comes from the close proximity of DDE residues in the three-dimensional structures of the catalytic core fragment of MuA transposase (Rice and Mizuuchi, 1995) and the observation that MuA DDE mutants are suppressed by Mn^{2+} (Baker and Luo, 1994; Kim *et al.*, 1995). Based on the phenotype of IS10 transposase DDE mutants, and the role that DDE residues play in other phosphoryl transfer reactions, it is very likely that a single active site participates in both excision and strand transfer reactions in Tn*10* transposition. Furthermore, evidence has been provided that a single IS10 transposase monomer performs all three chemical steps at a single transposon end (Bolland and Kleckner, 1996).

Divalent metal ions can also play important structural roles in protein-mediated phosphoryl transfer reactions involving DNA. In Mu transposition, the formation of the synaptic complex is dependent on a divalent metal ion (Mizuuchi *et al.*, 1992). In addition, the stability of the analogous complex in Tn*10* transposition is increased in the presence of a divalent metal ion (Sakai *et al.*, 1995).

In order to learn more about the various steps in Tn*10* transposition and the roles that divalent metal ions play in these steps, we have looked at the divalent metal ion requirements at distinct stages in Tn*10* transposition and examined previously identified IS10 transposase mutants for possible defects in divalent metal ion interactions. We demonstrate that (i) excision and integration reactions have significantly different Mg^{2+} requirements, (ii) double strand cleavage events at a pair of transposon ends can be completely uncoupled by limiting the Mg^{2+} concentration, (iii) substituting Mn^{2+} for Mg^{2+} relaxes target specificity in a wild-type reaction and suppresses transposase mutants that are defective in integration but not excision, and (iv) a transposase mutant with altered target specificity has a requirement for a higher Mg^{2+} concentration than wild-type for strand transfer.

Results

In vitro reactions at suboptimal Mg^{2+} concentrations

We have looked at the Mg^{2+} requirements at different stages of Tn*10* transposition by performing reactions at suboptimal Mg^{2+} concentrations and analysing the product compositions in these reactions. Reactions were performed using wild-type transposase and a supercoiled plasmid substrate containing a mini-Tn*10* *KanR* element (see Materials and methods). Transposition products were detected by Southern blot analysis using ^{32}P-labelled substrate plasmid as a probe. Under optimal conditions (5 mM Mg^{2+}), several products were observed including transposon circle (TnO), topologically complex strand transfer products (TC-STP), excised transposon (ETF), a cryptic end ETF (*ETF), donor backbone and linearized substrate (Figure 2). TnO and TC-STP are intramolecular strand transfer products previously described in Benjamin and Kleckner (1989, 1992). At this Mg^{2+} concentration, the ratio of ETF to TnO was slightly less than one. In contrast, at a Mg^{2+} concentration of 1.2 mM, this ratio increased to $\geqslant$20 without a significant drop in transposon excision, as indicated by equivalent levels of donor backbone in the two reactions. Interestingly, the differential elimination of strand transfer at low Mg^{2+} concentrations mimics the effect of a specific class of IS10 transposase mutants which we refer to as $Exc^{+}Int^{-}$. These mutants were identified on the basis that they retained the wild-type capacity to induce host SOS functions in the presence of transposon ends but could not promote transposition and were subsequently shown to accumulate an excised transposon intermediate. The identification of these mutants identified a major breakpoint in the Tn*10* transposition reaction. Remarkably, the same breakpoint can be achieved in the wild-type reaction by reducing the Mg^{2+} concentration.

There is normally a temporal separation of double strand cleavage events at a pair of ends in Tn*10* transposition (Haniford and Kleckner, 1994; Sakai *et al.*, 1995). A second effect of decreasing Mg^{2+} was that double strand

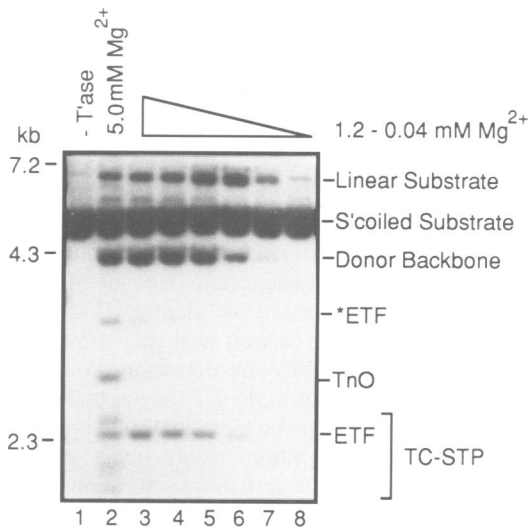

Fig. 2. Transposition products formed at suboptimal Mg^{2+} concentrations with wild-type transposase. Reactions were performed with the mini-Tn*10 KanR* plasmid under standard conditions with the exception that Mg^{2+} concentrations were varied: lane 2, 5 mM; lane 3, 1.25 mM; lane 4, 0.6 mM; lane 5, 0.3 mM; lane 6, 0.15 mM; lane 7, 0.08 mM; lane 8, 0.04 mM. After reactions were terminated, they were subjected to electrophoresis on a 1.1% agarose gel and species were detected by Southern blot analysis using the substrate plasmid, ^{32}P-labelled by hexopriming, as probe. Positions of transposon circles (TnO), topologically complex strand transfer products (TC-STP), excised transposon fragment (ETF), an ETF generated by the use of one inside end and a cryptic end (*ETF), linear substrate, donor backbone and supercoiled substrate are indicated.

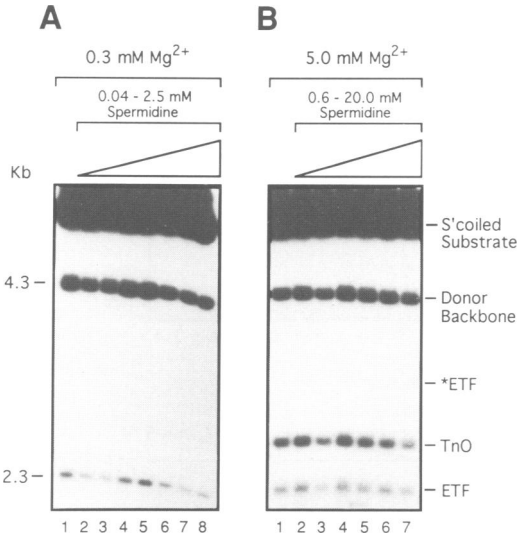

Fig. 3. Effects of spermidine on excision and strand transfer reactions performed with wild-type transposase. (**A**) Standard *in vitro* transposition reactions were performed using a concentration of Mg^{2+} (0.3 mM) that is optimal for excision, but does not permit strand transfer. Spermidine was included in the reactions shown in lanes 2–8. In these reactions, spermidine concentrations were decreased by 2-fold increments starting from 2.5 mM (lane 8) to 0.04 mM (lane 2). (**B**) Reactions were performed as in (A) except that the optimal Mg^{2+} concentration for strand transfer (5.0 mM) was used, and spermidine concentrations were varied starting from 20.0 mM (lane 7) and decreased in 2-fold increments to 0.6 mM (lane 2). The improved resolution of species in (A) and (B) relative to other experiments presented in this work is a result of increasing the voltage during electrophoresis and the total time of electrophoresis. Species were detected as in Figure 2.

cleavage events at the two transposon ends were increasingly uncoupled. This is indicated by the increase in the ratio of linearized substrate to donor backbone relative to that observed at the optimal Mg^{2+} concentration (compare lane 2 with lanes 6 and 7 in Figure 2). In fact, at a Mg^{2+} concentration of 0.08 mM, only single end cleavage events were detected. Specific mutations at the terminal 3 bp of the outside end of IS10 Right (Haniford and Kleckner, 1994) and substituting Mn^{2+} for Mg^{2+} (Bolland and Kleckner, 1995) are other factors which previously have been noted to exaggerate the uncoupling between single and double end cleavage events.

In order to evaluate the possibility that the inability to carry out strand transfer at low Mg^{2+} concentrations might reflect a non-specific effect related to charge neutralization, we have looked at the ability of spermidine to suppress the strand transfer defect observed at a suboptimal Mg^{2+} concentration. *In vitro* reactions were performed with wild-type transposase at either 0.3 or 5.0 mM Mg^{2+}, and the reactions were supplemented with the indicated amounts of spermidine (Figure 3A and B). While transposon excision occurred at similar levels in the two sets of reactions, as reflected by the amount of donor backbone and ETF formed, high levels of TnO were only observed in the reactions containing 5 mM Mg^{2+}. The result from Figure 3A indicates that spermidine does not suppress the strand transfer defect, suggesting that this defect is not related to non-specific charge neutralization. The result from Figure 3B indicates that at the spermidine concentrations tested there was no inhibition of strand transfer.

In vitro reactions with Ca^{2+} and Mg^{2+}

We have also analysed the ability of Ca^{2+} to function in the excision reaction. Ca^{2+} does not support excision (or strand transfer) on its own. It does, however, stabilize the paired end complex, indicating that it can play an important structural role (Sakai *et al.*, 1995). In the experiment shown in Figure 4A, reactions were performed in the presence of Mg^{2+}(0.15 mM) and Ca^{2+} (0.02–1.2 mM). At this Mg^{2+} concentration, a high degree of uncoupling of cleavage events at the two transposon ends is observed. The results showed that addition of Ca^{2+} further increased the extent of this uncoupling, demonstrating that Ca^{2+} only inhibited the cleavage reaction as opposed to stimulating it. This experiment also shows that the uncoupling of double strand cleavage events at 0.15 mM Mg^{2+} is not a non-specific effect related to charge neutralization.

The ability to separate excision from strand transfer at low Mg^{2+} concentrations also permitted us to investigate the ability of Ca^{2+} to function specifically in strand transfer (Figure 4B). Reactions were carried out at an Mg^{2+} concentration which supports optimal levels of excision but not strand transfer. After sufficient time to allow for excision, Ca^{2+} was added to some samples and then varying amounts of Mg^{2+} were added. In the absence of Ca^{2+}, strand transfer products were detected at final Mg^{2+} concentrations ranging from 1.0 to 5.3 mM (lanes 8–11) while, in the presence of Ca^{2+}, strand transfer products were not detected until a final Mg^{2+} concentration of 5.3 mM (lane 18). At this point, the level of strand transfer products was only ~50% that of the reaction in which

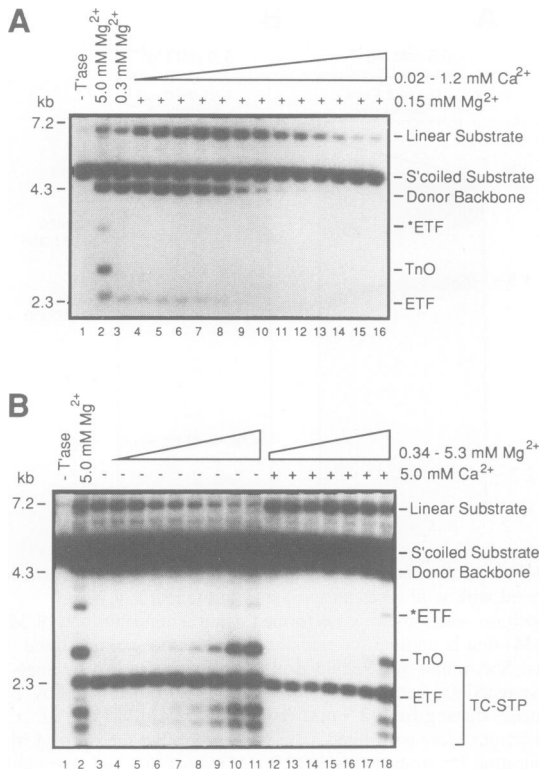

Fig. 4. Divalent metal ion competition experiments with wild-type transposase. (**A**) Reactions were performed as in Figure 2 except that, where indicated, both Mg^{2+} and Ca^{2+} were included. In reactions where both Mg^{2+} and Ca^{2+} were present, the concentration of Mg^{2+} was 0.15 mM, which is just above the minimal amount required for transposon excision, while Ca^{2+} concentrations varied starting from 1.25 mM (lane 16) and decreasing by 2-fold increments (even-numbered lanes) to 0.02 mM (lane 4), or varied starting from 0.94 mM (lane 15) and decreasing by 2-fold increments (odd-numbered lanes) to 0.03 mM (lane 5). (**B**) Reactions were initiated in the presence of 0.3 mM Mg^{2+}, which is optimal for excision but does not support strand transfer. After 2 h, Ca^{2+} was added at a concentration of 5 mM to reactions in lanes 12–18 and, after an additional 1.5 h, Mg^{2+} was added to different final concentrations. Mg^{2+} was added, starting at 5.0 mM (lanes 11 and 18) and decreasing by 2-fold increments to 0.04 mM (lane 4) and 0.08 mM (lane 12). The range of final Mg^{2+} concentrations is shown. The reaction in lane 3 received 0.3 mM Mg^{2+} only. Species were detected as in Figure 2.

Ca^{2+} was omitted (lane 11). This experiment indicates that Ca^{2+} does not support strand transfer. In fact, it is likely that Ca^{2+} competes for divalent metal ion binding sites in transposase that are necessary for strand transfer, since the addition of another cation, spermidine, did not inhibit strand transfer (see Figure 3B). In contrast to Tn*10* transposition, Ca^{2+} does support strand transfer in Mu transposition (Savilahti *et al.*, 1995).

Mn^{2+} relaxes target specificity

Both excision and strand transfer reactions take place in the presence of Mn^{2+}. However, at Mn^{2+} concentrations above the wild-type optimum, substrate molecules containing a nick on the transferred strand at each transposon–donor junction (Bolland and Kleckner, 1995) and the single end break species (Bolland and Kleckner, 1996) accumulate to levels significantly higher than that observed for wild-type reactions at 5 mM Mg^{2+}. We were interested in determining if Mn^{2+} had any other significant effects on the *in vitro* Tn*10* transposition reaction and have looked at the effect of Mn^{2+} on Tn*10* target specificity. We addressed this question by performing low resolution mapping of integration sites in TnOs generated by wild-type transposase in the presence of either Mg^{2+} or Mn^{2+}. Integration sites were mapped by digesting gel slices containing TnOs with *Bam*HI and then running out the digestion products in a second dimension. The sizes of the fragments produced reveal the approximate positions of target sites, since the formation of TnOs involves the inversion of transposon sequences to one side of the target site with respect to the rest of the element (Figure 5A).

When the wild-type reaction was performed in the presence of Mg^{2+}, four different digestion products were detected as shown in Figure 5B. F1 (arrow marked by *) was the predominant digestion product and is indicative of the majority of integration events being at a target site(s) located between a transposon terminus and the closest *Bam*HI site. The less abundant species (unmarked arrows) are indicative of integration events at target sites located between *Bam*HI sites. In the presence of Mn^{2+}, the same digestion products as above were observed. However, the relative amounts of these products differed from the Mg^{2+} reaction; F1 was still a prominent product but the level of other products increased significantly relative to F1. Furthermore, in the presence of Mg^{2+}, CY134, which is a transposase mutant known to alter target specificity *in vivo* (designated ATS; Bender and Kleckner, 1992), produced a similar pattern of digestion products to that observed in the wild-type reaction with Mn^{2+}. Taken together, these results indicated that at an Mn^{2+} concentration close to the wild-type optimum, which is ~0.1 mM (see Figure 7), the target specificity of wild-type transposase is relaxed. Thus, substituting Mn^{2+} for Mg^{2+} in a reaction with wild-type transposase mimics the effect of ATS mutations.

Mn^{2+} suppresses Exc^+Int^- mutants

Exc^+Int^- IS10 transposase mutants mediate Tn*10* excision at wild-type levels but do not promote strand transfer. We have noted previously that Exc^+Int^- mutations can be suppressed to varying degrees by introducing a second amino acid substitution (CY134) that on its own confers an ATS phenotype (Junop *et al.*, 1994). Based on the above observation that Mn^{2+} also confers an ATS phenotype, we were interested in determining if Mn^{2+} can also suppress Exc^+Int^- mutations. *In vitro* reactions were carried out with six different Exc^+Int^- mutants in the presence of Mg^{2+}(5 mM) or Mn^{2+} (0.15 mM) (Figure 6). Whereas none of the mutants produced detectable levels of TnO at 5 mM Mg^{2+}, all of the mutants were able to make TnO in the presence of 0.15 mM Mn^{2+}. TnO levels ranged from ~70 (for PS167) to 5% (for RH243) of that produced by wild-type at 5 mM Mg^{2+}.

We looked in more detail at the optimal metal ion requirements for all of the Exc^+Int^- mutants shown in Figure 6. Parallel experiments were performed with all of the mutants and the results did not differ significantly, so only data for one mutant, DE100, are presented (Figure 7). The optimal Mn^{2+} concentration for wild-type is close to 0.15 mM (lane 5), as above and below this concentration TnO formation decreased. Maximal suppression of DE100 occurred at approximately the same Mn^{2+} concentration (lane 11), indicating that this mutant has the same Mn^{2+}

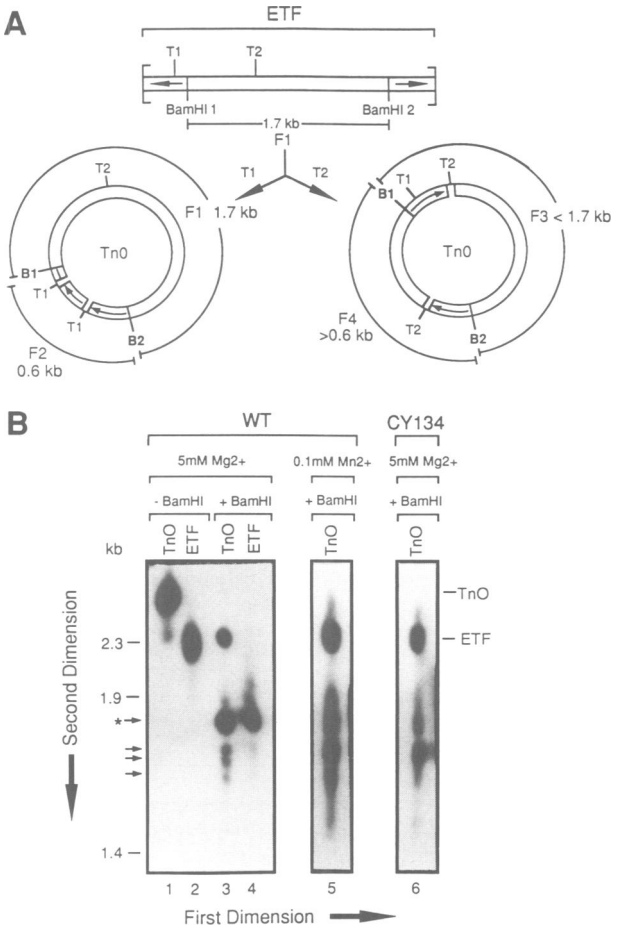

Fig. 5. Mapping of target sites by two-dimensional gel electrophoresis. (**A**) Schematic of the products expected after *Bam*HI digestion of ETFs and TnOs in reactions carried out with wild-type transposase under standard conditions. T1 and T2 represent hypothetical target sites. The *Bam*HI sites are located 300 bp from the transposon termini and the entire transposon is 2319 bp in length. Digestion of the excised transposon (ETF) with *Bam*HI results in the formation of a 1702 bp fragment (F1). Digestion with *Bam*HI of the transposon circle formed when T1 is used as a target site also produces the F1 fragment as well as a second fragment (F2) which is 617 bp; fragments F1 and F2 are produced regardless of where the target site is positioned in the interval between a *Bam*HI site and the closest transposon terminus. The size of the fragments produced by *Bam*HI digestion of TnOs formed when the target site is located in the interval between *Bam*HI sites will depend upon the exact position of the target site. In the example shown, digestion with *Bam*HI of a TnO formed when T2 is used as a target site produces a fragment (F3) which is smaller than 1.7 kb and a fragment (F4) which is larger than 0.6 kb. (**B**) Mapping of target sites used in TnOs was carried out as described in Materials and methods. The positions of ETF and TnO following electrophoresis in the first and second dimensions are shown. * indicates the 1.7 kb fragment expected for *Bam*HI digestion of TnOs in which a target site used for integration is located between a *Bam*HI site and the closest transposon terminus. Unlabelled arrows indicate the positions of fragments indicative of TnOs in which the target sites used for integration are located between the two *Bam*HI sites. In lanes 3, 5 and 6, the band with a mobility of ~2.3 kb results from partial digestion of TnOs. Products were detected by Southern blot analysis using the large *Bam*HI fragment from the mini-Tn*10* *KanR*, ^{32}P-labelled by hexopriming, as probe.

optimum as wild-type. At Mn^{2+} concentrations >1.2 mM there was a significant drop in TnO formation for DE100 with only a moderate drop in ETF formation. Both ETF and TnO formation dropped off to similar levels in the

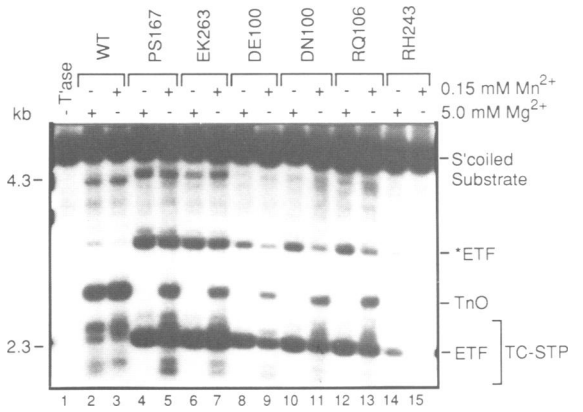

Fig. 6. Effect of Mn^{2+} on the integration defect of Exc^+Int^- transposase proteins. Six different Exc^+Int^- mutants were examined in reactions containing either 0.15 mM Mn^{2+} or 5 mM Mg^{2+}. The respective divalent metal ion concentrations used represent the optimal concentrations of these ions for TnO formation in both wild-type and mutant reactions. Species were detected as described in Figure 2.

wild-type reaction under the same conditions. Increasing the Mg^{2+} concentration above the wild-type optimum affected DE100 and wild-type reactions in the same way as increasing the Mn^{2+} concentration (Figure 7 and data not shown).

Mg^{2+} requirements for strand transfer with CY134

The mutation CY134 relaxes target sequence requirements for Tn*10* integration. Since Mn^{2+}, which has a concentration optimum some 50-fold lower than Mg^{2+}, can relax target specificity, we were interested in determining if relaxation of target specificity in CY134 might be related to alterations in Mg^{2+} binding properties. Two experimental approaches were used to examine the Mg^{2+} requirements for CY134 in strand transfer. In the experiment in Figure 8, reactions were performed at an Mg^{2+} concentration which supports excision but not strand transfer and then Ca^{2+} was added to 5 mM followed by the addition of varying amounts of Mg^{2+}. The results indicate that with CY134 a higher concentration of Mg^{2+} was required to carry out strand transfer relative to wild-type transposase (compare lanes 8 and 9 with lanes 17 and 18). In a second experiment, an Mg^{2+} titration was performed as in Figure 2. A higher concentration of Mg^{2+} was required to form TnO in the CY134 reaction compared with the wild-type reaction (data not shown). These experiments suggest that relaxation of target specificity by CY134 is not a consequence of higher affinity divalent metal ion binding. Also, the amount of Mg^{2+} required to see excision with CY134 does not differ significantly from wild-type; therefore, this alteration in Mg^{2+} affinity is confined to a specific Mg^{2+}-requiring step in strand transfer, further indicating distinct roles for Mg^{2+} at different stages in Tn*10* transposition.

Discussion

Effects of limiting Mg^{2+} on Tn10 transposition in vitro

We have demonstrated that, by limiting the amount of Mg^{2+} in the *in vitro* Tn*10* transposition reaction, transposition can be affected in at least two distinct steps, including

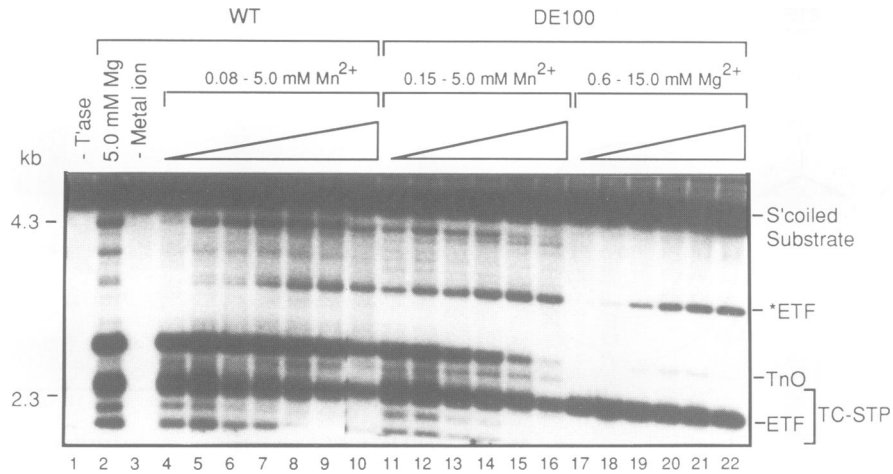

Fig. 7. Effect of Mn^{2+} on reactions performed with wild-type and $Exc^{+}Int^{-}$ transposase proteins. Reactions were performed as in Figure 2 except that, where indicated, Mg^{2+} was replaced with Mn^{2+} and in some reactions Mg^{2+} concentrations higher than the wild-type optimum were used. Mn^{2+} concentrations were decreased by 2-fold increments starting from 5.0 mM (lane 10) to 0.08 mM (lane 4) and 5.0 mM (lane 16) to 0.15 mM (lane 11). Mg^{2+} concentrations were decreased by 2-fold increments starting at 10.0 mM (lane 21) to 0.6 mM (lane 17). The Mg^{2+} concentration in lane 22 was 15 mM. Species were detected as described in Figure 2.

(i) the conversion of the single end break intermediate to the excised transposon intermediate (or ETF) and (ii) the conversion of the ETF to a strand transfer intermediate (TnO). Furthermore, the uncoupling of strand transfer from transposon excision occurs at Mg^{2+} concentrations (0.6–1.2 mM) significantly above those at which uncoupling of donor cleavage events occurs (0.08–0.16 mM). This indicates that there is a block specifically in TnO formation at the higher Mg^{2+} concentrations. The observation that neither spermidine nor Ca^{2+} suppress the defects described above indicates that the effects of limiting Mg^{2+} are related to specific roles of Mg^{2+} in Tn*10* transposition as opposed to a non-specific effect such as charge neutralization.

The breakpoints in the reaction identified here by Mg^{2+} titrations have previously been identified genetically and biochemically. The delay in double strand cleavage at the second end is greatly exaggerated by specific mutations in the terminal three nucleotides of the outside end of IS10 Right (Haniford and Kleckner, 1994; Sakai *et al.*, 1995). $Exc^{+}Int^{-}$ transposase mutations accumulate ETFs but do not form TnOs (Haniford *et al.*, 1989). These classes of mutations identify moieties in the synaptic complex that are important in the transition from one step in the reaction to the next. The observation that these breakpoints can also be achieved by limiting Mg^{2+} emphasizes the importance of Mg^{2+} in these transitions and suggests that the above classes of mutations might play a role in Mg^{2+} interactions. Defining the mechanisms which regulate the transition from step to step in the reaction is central to our understanding of the transposition process.

There is evidence that transposable elements other than Tn*10* also have different divalent metal ion requirements at different steps. In Mu transposition, Ca^{2+} can support strand transfer but not donor cleavage (Savilahti *et al.*, 1995). This result provides strong evidence for a conformational change in the active site in the transition from donor cleavage to strand transfer. In the human immunodeficiency virus (HIV)-1 integration reaction, viral processing is observed at divalent metal ion concentrations which do not support strand transfer (Vincent *et al.*, 1993).

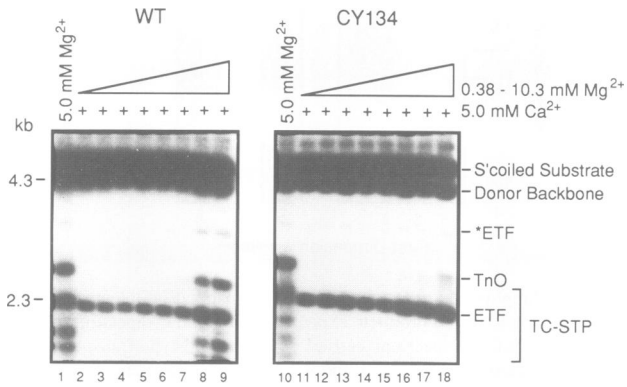

Fig. 8. Divalent metal ion competition experiments with CY134. Reactions were performed with either wild-type or CY134 transposase proteins as in Figure 4B. Briefly, reactions were initiated in the presence of 0.3 mM Mg^{2+}. After 2 h, Ca^{2+} was added to a final concentration of 5 mM and, after an additional 1.5 h, Mg^{2+} was added to different final concentrations. Mg^{2+} was added starting at 10.0 mM (lanes 18 and 9) and decreasing in 2-fold increments to 0.08 mM (lanes 10 and 2). The range of final Mg^{2+} concentrations is shown. Species were detected as in Figure 2.

Information pertaining to the number, position(s) and type(s) of divalent metal ion binding site(s) in IS10 transposase has not yet been obtained. However, evidence has been provided that a single active site in a transposase monomer performs all three of the chemical steps in which a single transposon end participates (i.e. cleavage of transferred and non-transferred strands and strand transfer) and that these steps are all dependent on a suitable divalent metal ion (Bolland and Kleckner, 1996). It does not appear likely that double strand cleavage events at a pair of ends are mechanistically coupled, as the amount of time between cleavage events is typically longer than the amount of time required for the first event (Sakai *et al.*, 1995). In this case, the uncoupling of double strand cleavage events at a pair of transposon ends at low Mg^{2+} concentrations

is most easily explained by there being insufficient Mg^{2+} available to bind the active sites of two different transposase monomers in the synaptic complex or ancillary divalent metal ion sites whose occupancy influences active site function. We have also shown that at Mg^{2+} concentrations just sufficient to promote transposon excision, Ca^{2+} has an inhibitory effect on excision, i.e. the ratio of single to double end break product increases significantly relative to a reaction performed in the absence of Ca^{2+}. It is likely that this indicates that Ca^{2+} has the ability to compete with Mg^{2+} for binding to either the active site or an ancillary site. It is of interest to note that the catalytic activity of *Eco*RI but not *Eco*RV is inhibited in similar types of Mg^{2+}/Ca^{2+} mixing experiments (Vipond *et al.*, 1995). These results, together with structural data (Rosenberg, 1991; Kostrewa and Winkler, 1995), have provided evidence for one and two divalent metal ion phosphoryl transfer mechanisms for cleavage, respectively.

If a single monomer of transposase catalyses both excision and strand transfer events for a single end, as proposed by Bolland and Kleckner (1996), then how might the uncoupling between excision and strand transfer occur at limiting Mg^{2+} concentrations? One possibility is that the affinity of the active site for Mg^{2+} could be lower at the strand transfer stage compared with the donor cleavage stage of the reaction. In the transition from donor cleavage to strand transfer, flanking donor DNA has to be removed from the active site and replaced with target DNA (J.Sakai and N.Kleckner, personal communication). If the flanking DNA provides important ligands for Mg^{2+} binding, then the loss of these ligands would reduce the level of Mg^{2+} occupancy in the active site. Assuming that the replacement of flanking DNA with target DNA does not restore the affinity of the active site for Mg^{2+} to the pre-excision level, then reducing the Mg^{2+} concentration would be expected to have a significant influence on the efficiency of strand transfer. A precedent for DNA substrates providing important ligands for divalent metal ion binding in phosphoryl transfer reactions comes from structural studies on Klenow fragment polymerase (Beese and Steitz, 1991), rat β polymerase (Pelletier *et al.*, 1994), *Eco*RV (Winkler *et al.*, 1993) and *Eco*RI (Rosenberg, 1991). Alternatively, there might exist a separate Mg^{2+} binding site in transposase which functions specifically in target interactions. If this site were to have a lower affinity for Mg^{2+} than the catalytic core, then strand transfer would be less efficient at suboptimal Mg^{2+} concentrations compared with steps in the reaction that do not involve the target DNA. Interestingly, in the case of *Eco*RV, it has been shown that disruption of the catalytic core domain by mutation of metal ion ligands does not influence the ability of the protein to bind a cognate site in an Mg^{2+}-dependent manner, suggesting a role for Mg^{2+} in a step separate from catalysis (Jeltsch *et al.*, 1995). Mg^{2+} could provide critical bridging interactions between the target site and transposase necessary to stabilize the specific target complex. A role for Mg^{2+} in target specificity could be achieved if these bridging interactions are only formed when a selective class of target DNA sequences are bound. This general model has been proposed by Jeltsch *et al.* (1995) to explain the DNA binding specificity retained by the above *Eco*RV mutant.

A mechanism for uncoupling steps in Tn10 transposition

Tn*10* transposition can be uncoupled at three different steps, resulting in the accumulation of doubly nicked (cleavage only on the transferred strands) (Bolland and Kleckner, 1995), single end break (Haniford and Kleckner, 1994; Sakai *et al.*, 1995; Bolland and Kleckner, 1996; this work) and excised transposon intermediates (Haniford *et al.*, 1989; this work). Is there a common event that could account for the accumulation of all of these species? One possibility is that there is a release of divalent metal ion(s) from the active site after each of the three catalytic steps are performed on a single end, followed by a conformational change in the synaptic complex which is required for the next step. In this case, the use of a divalent metal ion above its optimum might specifically inhibit cleavage of the non-transferred strand and strand transfer, because in both reactions the higher concentration of divalent metal ion would shift the binding equilibrium towards the bound state blocking progression to the next step. In fact, an accumulation of both doubly nicked and single end break species is observed in wild-type reactions performed at Mn^{2+} concentrations above the optimum (Bolland and Kleckner, 1995, 1996). Also, results presented in this work demonstrate that, at Mg^{2+} and Mn^{2+} concentrations above their respective optima, strand transfer is more strongly inhibited than other steps in reactions with the mutant DE100. It may also be significant that transposase mutants which confer a hypernicking phenotype under standard reaction conditions also inhibit strand transfer (Haniford *et al.*, 1989; Bolland and Kleckner, 1995). This is consistent with the idea that both cleavage of the non-transferred strand and strand transfer are dependent on a related conformational change in the synaptic complex.

Effects of Mn^{2+} on Tn10 transposition

In this work, we have identified two additional effects of Mn^{2+} on Tn*10* transposition. First, Mn^{2+} relaxes target sequence requirements for Tn*10* integration. This indicates that a divalent metal ion plays an important role in establishing target specificity in Tn*10* transposition. Second, Mn^{2+} is capable of suppressing the integration defect in $Exc^{+}Int^{-}$ mutants. Since both of these effects are observed at Mn^{2+} concentrations at, or very close to, the wild-type optimum, it is likely that alterations in the affinities of divalent metal ions for transposase are not responsible for the above phenomena. By comparison, it has been shown that MuA transposase mutants which are expected to influence Mg^{2+} binding directly are suppressed by Mn^{2+}, but only at concentrations substantially above the wild-type optimum (Baker and Luo, 1994; Kim *et al.*, 1995).

Mn^{2+} has been observed to relax sequence specificity in other phosphoryl transfer reactions including those mediated by ASLV (Katzman *et al.*, 1989) and HIV-1 (Drelich *et al.*, 1992) integrase proteins and restriction endonucleases *Eco*RI (Hsu and Berg, 1978) and *Eco*RV (Vermote and Halford, 1992). For *Eco*RI and *Eco*RV, there is strong evidence suggesting that sequence-specific binding induces a conformational change in the enzyme–substrate complex which is required for catalysis. For *Eco*RV, an increased binding affinity for Mn^{2+} relative to

Mg^{2+} makes the reaction less dependent on a conformational change which is linked to cognate site binding and required to establish a high affinity divalent metal ion binding site. The occupancy of this site is essential for catalysis (Winkler *et al.*, 1993). For *Eco*RI, a conformational change linked to cognate site binding is thought to position substrate and divalent metal ion properly in the active site for catalysis. The larger atomic radius of Mn^{2+} and/or its greater versatility in ligand interactions relative to Mg^{2+} is thought to make catalysis less dependent on this conformational change (Heitman, 1992). It follows that, in both systems, factors which decrease the dependence of catalysis on the conformational change will relax specificity. The relaxation of target specificity in Tn*10* transposition by Mn^{2+} could similarly reflect an intricate coupling between specific target site binding and catalysis of strand transfer.

We have shown previously that Exc^+Int^- mutants are suppressed by a second site mutation that on its own relaxes target specificity (Junop *et al.*, 1994). The observation here that Mn^{2+} also relaxes specificity and suppresses Exc^+Int^- provides confirmation that the two phenotypes are inextricably linked. Based on the above models for how relaxation of target specificity might be achieved, we suggest that Exc^+Int^- mutants are defective in specific target site binding and/or the ability to undergo the conformational change linked to specific target site binding. Either of these defects would be suppressed by making the reaction less dependent upon the coupling between specific target site binding and catalysis of strand transfer (i.e. Mn^{2+} or the mutation, CY134). The fact that amino acid substitutions in a large number of residues in transposase result in an Exc^+Int^- phenotype is suggestive of a defect in a step involving a conformational change (Haniford *et al.*, 1989). It has been proposed previously that CY134 might predispose transposase to a conformation which is active for strand transfer, as the types of substitutions at ATS positions (amino acids 134 and 249) that retain a wild-type phenotype or confer an ATS phenotype argue against these positions having a direct role in divalent metal ion binding (Bender and Kleckner, 1992). Our results are consistent with the effect of ATS mutations being conformational as oppossed to increasing the affinity for divalent metal ions, as CY134 exhibits a decreased affinity for Mg^{2+} relative to wild-type.

In summary, we have identified breakpoints in the Tn*10* transposition reaction which are extremely sensitive to the concentration of Mg^{2+} in the reaction. In addition to the amount of Mg^{2+} being important for the transition from step to step, the nature of the divalent metal ion also influences the outcome of the reaction as substituting Mn^{2+} for Mg^{2+} relaxes target specificity and suppresses Exc^+Int^- transposase mutants. Determining the molecular basis for these effects is expected to contribute greatly to our understanding of Tn*10* transposition and possibly other transposition reactions, including those mediated by the retroviral integrases where some of the same effects have been observed.

Materials and methods

Plasmids

Plasmid pNK2853 contains the IS10 transposase gene fused to a T7 promoter (Haniford *et al.*, 1991). IS10 transposase mutants originally isolated in pDH10 (Haniford *et al.*, 1989) were cloned on *Nhe*I–*Stu*I fragments into an appropriately prepared pNK2853 backbone to create pDH151 (DN100), pDH152 (DE100), pDH156 (RQ106), pDH157 (CY134), pDH158 (CW134), pDH160 (PS167), pDH161 (RH243) and pDH162 (EK263).

Plasmid pNK1182 contains a mini-Tn*10 KanR* transposon comprised of the terminal 300 bp of the inside end of IS10 Right repeated in inverted orientation on either side of the kanamycin resistance element from Tn*903* (Morisato and Kleckner, 1987).

Protein purification

Wild-type and mutant IS10 transposase proteins were purified from BL21(DE3)/pLysS transformed with pNK2853 (and derivatives) as described by Chalmers and Kleckner (1994) with the following modification: during the final step of the purification, soluble transposase was applied to a Superose 12 gel filtration column equilibrated with modified buffer B containing 2 M NaCl, 20 mM Triton X-100 instead of 2 M NaCl, 50 mM Triton X-100. Protein concentrations were determined by the BCA assay (Chalmers and Kleckner, 1994). Typical yields from 5 g (wet weight) of cells were in the range of 0.25–0.5 mg/ml.

In vitro transposition reactions

Transposition reactions were carried out under standard conditions as described in Chalmers and Kleckner (1994), except that in some cases $MgCl_2$ concentrations were varied, $MnCl_2$ was used in place of $MgCl_2$ or both $CaCl_2$ and $MgCl_2$ were included. Different concentrations of divalent metal ions were prepared by serial dilution of 1.0 M stock solutions. Briefly, reactions were carried out by adding 2 μl of transposase (15 ng or 330 fmol), diluted in a buffer containing 25 mM TES (pH 7.5), 10 mM dithiothreitol (DTT), 2 mM EDTA (pH 7.5), 0.5 M NaCl, 50% glycerol, and 1 mg/ml bovine serum albumin (BSA), in a final reaction volume of 100 μl containing 20 mM Tris–HCl (pH 7.5), 5 mM $MgCl_2$, 35 mM ammonium sulfate, 10 mM DTT, 1 mM spermidine, 15% (v/v) glycerol, 50 μg/ml BSA and 0.5 μg (230 fmol) of pNK1182. In all experiments, total reaction times were 5 h at 30°C and reactions were terminated by the addition of 12.5 μl of 300 mM EDTA, 2.5% SDS followed by digestion with 1 μl of proteinase K (1 mg/ml) for 30 min at 55°C. DNA was precipitated with ethanol and then resuspended in 10 μl of water plus 10 μl of gel loading dye [30% sucrose, 10 mM Tris–HCl (pH 8.0), 1 mM EDTA, 0.05% bromphenol blue and 0.1% SDS]. Electrophoresis was carried out on a 1.1% agarose gel (0.5 cm×13 cm×25 cm) in 1× TBE buffer at 2.8 V/cm for 16 h or at 3.5 V/cm for 20 h. Species were detected by Southern blot analysis in which either the whole substrate plasmid or a *KanR* fragment from the mini-Tn*10 KanR* in pNK1182 was used as probe.

Mapping of target sites within mini-Tn10 KanR

Standard transposition reactions were carried out with purified transposase proteins and the pNK1182 substrate plasmid. Reaction mixtures were applied to a 1% low melting agarose gel (0.5 cm×13 cm×25 cm) run in 1× TBE buffer; electrophoresis was at 2.8 V/cm for 16 h. After staining with ethidium bromide, a gel slice containing ETF and TnO or only TnO was removed and subjected to two 30 min incubations in 50 volumes of TE (pH 7.6) at room temperature. The gel slice was then incubated in 10 volumes of 1× *Bam*HI restriction enzyme buffer (NEBL) for 30 min at 4°C. This buffer was then removed and replaced with 2–3 volumes of fresh *Bam*HI buffer along with 50 units of *Bam*HI enzyme, and the gel slice was incubated for 12 h at 37°C. The gel slice was placed in 50 volumes of TE (pH 7.6) at 4°C for 1 h and then inserted into a fresh 1.1% agarose gel (0.5 cm×13 cm×25 cm) which was run in 1× TBE buffer; electrophoresis in the second dimension was at 2.8 V/cm for 16 h. Species were detected by Southern blot analysis.

Quantification of product levels

Levels of products were quantified from autoradiograms by laser densitometry using a Gel Imager and Gel Print Tool Box Version 3.0 from Biophotonics. In order to ensure linearity, standards were loaded on each gel and multiple exposures were taken. Values were obtained from a standard curve (data not shown).

Acknowledgements

We would like to thank Dr G.Chaconas, Dr C.Brandl, Dr G.Shaw, Dr B.Lavoie, A.Kennedy and D.Hyduk for critical reading and helpful comments on the manuscript. We are also grateful to Dr N.Kleckner, J.Sakai and Dr R.Chalmers for providing plasmids and communicating

results prior to publication. This work was supported by a grant from the Medical Research Council of Canada to D.B.H. and by a Medical Research Council of Canada studentship to M.S.J.

References

Baker,T.A. and Luo,L. (1994) Identification of residues in Mu transposase essential for catalysis. *Proc. Natl Acad. Sci. USA*, **91**, 6654–6658.

Beese,L.S. and Steitz,T.A. (1991) Structural basis for the 3′-5′ exonuclease activity of *Escherichia coli* DNA polymerase I: a two metal ion mechanism. *EMBO J.*, **10**, 25–33.

Bender,J. and Kleckner,N. (1986) Genetic evidence that Tn*10* transposes by a nonreplicative mechanism. *Cell*, **45**, 801–815.

Bender,J. and Kleckner,N. (1992) IS10 transposase mutations that specifically alter target site recognition. *EMBO J.*, **11**, 741–750.

Benjamin,H.W. and Kleckner,N. (1989) Intramolecular transposition by Tn*10*. *Cell*, **59**, 373–383.

Benjamin,H.W. and Kleckner,N. (1992) Excision of Tn*10* from the donor site during transposition occurs by flush double-strand cleavages at the transposon termini. *Proc. Natl Acad. Sci. USA*, **89**, 4648–4652.

Bolland,S. and Kleckner,N. (1995) The two single-strand cleavages at each end of Tn*10* occur in a specific order during transposition. *Proc. Natl Acad. Sci. USA*, **92**, 7814–7818.

Bolland,S. and Kleckner,N. (1996) The three steps of Tn*10*/IS10 transposition involve repeated utilization of a single active site. *Cell*, **84**, 223–233.

Chalmers,R.M. and Kleckner,N. (1994) Tn*10*/IS10 transposase purification, activation, and *in vitro* reaction. *J. Biol. Chem.*, **269**, 8029–8035.

Craig,N.L. (1995) Unity in transposition reactions. *Science*, **270**, 253–254.

Craigie,R. and Mizuuchi,K. (1987) Transposition of Mu DNA: joining of Mu to target DNA can be uncoupled from cleavage at the ends of Mu. *Cell*, **51**, 493–501.

Davies,J.F.,II, Hostomska,Z., Hostomsky,Z., Jordan,S.R. and Matthews, D.A. (1991) Crystal structure of the ribonuclease H domain of Hiv-1 reverse transcriptase. *Science*, **252**, 88–95.

Dorner,L.F. and Schildkraut,I. (1994) Direct selection of binding proficient/catalytic deficient variants of *Bam*HI endonuclease. *Nucleic Acids Res.*, **22**, 1068–1074.

Drelich,M., Wilhelm,R. and Mous,J. (1992) Identification of amino acid residues critical for endonuclease and integration activities of HIV-1 IN protein *in vitro*. *Virology*, **188**, 459–468.

Halling,S.M. and Kleckner,N. (1982) A symmetrical six-base-pair target site sequence determines Tn*10* insertion specificity. *Cell*, **28**, 155–163.

Haniford,D.B. and Chaconas,G. (1992) Mechanistic aspects of DNA transposition. *Curr. Opin. Genet. Dev.*, **2**, 698–704.

Haniford,D.B. and Kleckner,N. (1994) Tn*10* transposition *in vivo*: temporal separation of cleavages at the two transposon ends and roles of terminal base pairs subsequent to interaction of ends. *EMBO J.*, **13**, 5847–5851.

Haniford,D.B., Chelouche,A. and Kleckner,N. (1989) A specific class of IS10 transposase mutants are blocked for target site interactions and promote formation of an excised transposon fragment. *Cell*, **59**, 385–394.

Haniford,D.B., Benjamin,H.W. and Kleckner,N. (1991) Kinetic and structural analysis of a cleaved donor intermediate and a strand transfer intermediate in Tn*10* transposition. *Cell*, **64**, 171–179.

Heitman,J. (1992) How the *Eco*RI endonuclease recognizes and cleaves DNA. *BioEssays*, **14**, 445–454.

Hsu,M. and Berg,P. (1978) Altering the specificity of restriction endonuclease: effect of replacing Mg^{2+} with Mn^{2+}. *Biochemistry*, **17**, 131–138.

Huisman,O., Errada,P.R., Signon,L. and Kleckner,N. (1989) Mutational analysis of IS10 outside end. *EMBO J.*, **8**, 2101–2109.

Jeltsch,A., Maschke,H., Selent,U., Wenz,C., Kohler,E., Connolly,B.A., Thorogood,H. and Pingoud,A. (1995) DNA binding specificity of the *Eco*RV restriction endonuclease is increased by Mg^{2+} binding to a metal ion binding site distinct from the catalytic center of the enzyme. *Biochemistry*, **34**, 6239–6246.

Junop,M.S., Hockman,D. and Haniford,D.B. (1994) Intragenic suppression of integration-defective IS10 transposase mutants. *Genetics*, **137**, 343–352.

Katzman,M., Katz,R.A., Skalka,A.M. and Leis,J. (1989) The avian retroviral integration protein cleaves the terminal sequences of linear viral DNA at the *in vivo* sites of integration. *J. Virol.*, **63**, 5319–5327.

Kennedy,A.K. and Haniford,D.B. (1996) Isolation and characterization of IS10 transposase separation of function mutants: identification of amino acids which are important for catalysis and interactions with DNA. *J. Mol. Biol.*, **256**, 533–547.

Kim,K., Namgoong,S.-Y., Jayaram,M. and Harshey,R. (1995) Step-arrest mutants of phage Mu transposase. *J. Biol. Chem.*, **270**, 1472–1479.

Kim,Y., Grable,J.C., Love,R., Greene,P.J. and Rosenberg,J.M. (1990) Refinement of *Eco*RI endonuclease crystal structure: a revised protein chain tracing. *Science*, **249**, 1307–1309.

Kleckner,N. (1989) Transposon Tn*10*. In Berg,D.E. and Howe,M.M. (eds), *Mobile DNA*. American Society for Microbiology, Washington, DC, pp. 335–374.

Kleckner,N., Chalmers,R., Kwon,D., Sakai,J. and Bolland,S. (1995) Tn*10* and IS10 transposition and chromosome rearrangements: mechanism and regulation *in vivo* and *in vitro*. *Curr. Top. Microbiol. Immunol.*, **204**, 49–82.

Kostrewa,D. and Winkler,F.K. (1995) Mg^{2+} binding to the active site of *Eco*RV endonuclease: a crystallographic study of complexes with substrate and product DNA at 2 Å resolution. *Biochemistry*, **34**, 683–696.

Kulkosky,J., Jones,K.S., Katz,R.A., Mack,J.P.G. and Skalka,A.M. (1992) Residues critical for retroviral integrative recombination in a region that is highly conserved among retroviral/retrotransposon integrases and bacterial insertion sequence transposases. *Mol. Cell. Biol.*, **12**, 2331–2338.

Mizuuchi,K. (1992a) Transpositional recombination: mechanistic insights from studies of Mu and other elements. *Annu. Rev. Biochem.*, **61**, 1011–1051.

Mizuuchi,K. (1992b) Polynucleotidyl transfer reaction in transpositional DNA recombination. *J. Biol. Chem.*, **267**, 21273–21276.

Mizuuchi,M., Baker,T.A. and Mizuuchi,K. (1992) Assembly of the active form of the transposase–Mu DNA complex: a critical control point in Mu transposition. *Cell*, **70**, 303–311.

Morisato,D. and Kleckner,N. (1987) Tn*10* transposition and circle formation *in vitro*. *Cell*, **51**, 101–111.

Pelletier,H., Sawaya,M.R., Kumar,A., Wilson,S.H. and Kraut,J. (1994) Structures of ternary complexes of rat DNA polymerase β, a DNA template–primer, and ddCTP. *Science*, **264**, 1892–1903.

Polard,P. and Chandler,M. (1995) Bacterial transposases and retroviral integrases. *Mol. Microbiol.*, **15**, 13–23.

Rice,P. and Mizuuchi,K. (1995) Structure of the bacteriophage Mu transposase core: a common structural motif for DNA transposition and retroviral integration. *Cell*, **82**, 209–220.

Rosenberg,J. (1991) Structure and function of restriction endonucleases. *Curr. Opin. Struct. Biol.*, **1**, 104–113.

Sakai,J., Chalmers,R.H. and Kleckner,N. (1995) Identification and characterization of a pre-cleavage synaptic complex that is an early intermediate in Tn*10* transposition. *EMBO J.*, **14**, 4374–4383.

Savilahti,H., Rice,P.A. and Mizuuchi,K. (1995) The phage Mu transpososome core: DNA requirements for assembly and function. *EMBO J.*, **14**, 4893–4903.

Selent,U., Ruter,T., Kohler,E., Liedtke,M., Thielking,V., Alves,J., Oelgeschlager,T., Wolfes,H., Peters,F. and Pingoud,A. (1992) A site-directed mutagenesis study to identify amino acid residues involved in the catalytic function of the restriction endonuclease *Eco*RV. *Biochemistry*, **31**, 4808–4815.

Surette,M.G., Buch,S.J. and Chaconas,G. (1987) Transpososomes: stable protein–DNA complexes involved in the *in vitro* transposition of bacteriophage Mu DNA. *Cell*, **49**, 253–262.

Van Gent,D.C., Groeneger,A.A.M.O. and Plasterk,R.H.A. (1992) Mutational analysis of the integrase protein of human immunodeficiency virus type 2. *Proc. Natl Acad. Sci. USA*, **89**, 9598–9602.

Vermote,C.L. and Halford,S.E. (1992) *Eco*RV restriction endonuclease: communication between catalytic metal ions and DNA recognition. *Biochemistry*, **31**, 6082–6089.

Vincent,K.A., Ellison,V., Chow,S.A. and Brown,P.O. (1993) Characterization of human immunodeficiency virus type 1 integrase expressed in *Escherichia coli* and analysis of variants with amino-terminal mutations. *J. Virol.*, **67**, 425–437.

Vipond,I.B., Baldwin,G.S. and Halford,S.E. (1995) Divalent metal ions at the active sites of the *Eco*RV and *Eco*RI restriction endonucleases. *Biochemistry*, **34**, 697–704.

Winkler,F.K. *et al.* (1991) The crystal structure of *Eco*RV endonuclease and of its complexes with cognate and non-cognate DNA fragments. *EMBO J.*, **12**, 1781–1795.

Received on November 9, 1995; revised on January 26, 1996